Paramagnetic centers in detonation nanodiamonds studied by CW and pulse EPR

A.V. Fionov [a,*], A. Lund [b], W.M. Chen [b], N.N. Rozhkova [c], I.A. Buyanova [b], G.I. Emel'yanova [a], L.E. Gorlenko [a], E.V. Golubina [a], E.S. Lokteva [a], E. Ōsawa [d], V.V. Lunin [a]

[a] Department of Chemistry, Moscow State University, Leninskije Gory, Moscow 119992, Russia
[b] Department of Physics, Chemistry and Biology, Linköping University, Linköping 58183, Sweden
[c] Institute of Geology, Karelian Research Centre RAS, Petrozavodsk 185610, Russia
[d] NanoCarbon Research Institute, Asama Research Extension Centre, Shinshu University, 3-15-1 Tokita, Ueda, Nagano 386-8567, Japan

ARTICLE INFO

ABSTRACT

Dispersed detonation nanodiamonds have been studied by continuous-wave (CW) and pulse EPR techniques. The spectrum of bulk radicals ($g = 2.0025 \pm 0.0002$, a Lorentz line shape with $\Delta H_{pp} = 0.95 \pm 0.05$ mT) dominated in CW EPR and prevented to record spectra from other paramagnetic species. The pulse EPR-spectrum was the superposition of the distorted P1-center spectrum with parameters ($g = 2.0025$, $A_{xx} = 2.57$ mT, $A_{yy} = 3.08$ mT, $A_{zz} = 4.07$ mT), the H1-center spectrum ($g = 2.0028$) and the single line ($g = 2.0025$, $\Delta H_{pp} = 0.40 \pm 0.05$ mT) from other centers which may be assigned to surface radicals. The concentration of P1-centers has been estimated by CW EPR as 2 ± 1 ppm N.

© 2010 Elsevier B.V. All rights reserved.

1. Introduction

The interest in nanodiamonds prepared by detonation techniques has increased in the last years [1–4]. These materials have small primary particles of diamond of several nanometer sizes together with various admixtures depending on the sample purification [5–7].

Detonation nanodiamonds have EPR spectra with $g = 2.0026$–2.0028, a Lorentz line shape with peak-to-peak derivative linewidths ΔH_{pp} varying from 0.75 to 1.2 mT and intensities up to 10^{20} spins/g [5–10]. Due to the short spin–lattice relaxation time (<10 μs [8]) of these radicals there is little microwave saturation at a microwave power up to 200 mW. The assignment of this spectrum to the dangling C–C bonds on the diamond cluster surface [5] or to the unpaired electrons located in the bulk of the nanodiamond particle [10,11] is under discussion.

A variety of paramagnetic defects has been discovered in natural and synthetic diamonds [12]. Detonation nanodiamond contains up to 2 wt.% nitrogen [13]. However, the concentration of paramagnetic nitrogen-containing defects in detonation nanodiamond is very low. According to theoretical considerations the nitrogen atoms are metastable within the core of nanodiamond [14,15]. Continuous-wave (CW) EPR was ineffective in the detection of paramagnetic substitutional nitrogen [16,17] but the use of pulse EPR allowed to record echo-detected EPR spectra of the P1-centers (carbon atom substituted by nitrogen) in the detonation nanodiamond [18,19]. The sintered detonation nanodiamond with increased crystallites size (8.5 nm) had a better pulse EPR-spectrum of the P1-centers [19,20]. However, detailed data of the magnetic resonance parameters as well as of the concentration of the P1-centers in detonation nanodiamonds are absent.

Detonation nanodiamonds have been used as effective and stable catalysts [21] and catalyst supports [22]. Therefore the study of the structure as well as the surface properties of such species is of great importance.

It was interesting to study detonation nanodiamonds by CW and pulse EPR techniques to detect paramagnetic species, to analyze their magnetic resonance parameters and to find the concentration of the P1-centers.

2. Materials and methods

The first nanodiamond sample (designated as ND#1) was prepared from the commercial detonation nanodiamond, produced by Gansu Goldstone Nano-Material Co., Ltd., Lanzhou, China [13]. This material was suspended in an excess of water and subjected to stirred-media of milling with 30 μm zirconia beads to prepare a stable colloidal solution of disintegrated primary single-nano buckydiamond (SNBD) particles. The preparation of the aqueous SNBD colloidal solution that is characterized by a narrow particle size distribution pattern with an average particle size value ~5 nm was described in detail elsewhere [23,24]. ND#1 powder was produced by drying of stable aqueous dispersions of SNBD at room temperature.

The second nanodiamond sample (designated as ND#2) was prepared at the Zababakhin All-Russia Research Institute of Technical Physics, Russian Federal Nuclear Center [25].

---

* Corresponding author. Fax: +7 495 9394575.
E-mail address: fionov@mail.ru (A.V. Fionov).

CW EPR measurements were made on a Bruker ELEXSYS E500-10/12 spectrometer. Spectra were recorded at suitable microwave power level to avoid saturation effects. The g-values were determined by comparison with the g-value of the 2,2,6,6-tetramethylpiperidine-N-oxyl (TEMPO) in 10^{-4} M toluene solution (g = 2.00611 [26]). To avoid systematic g-factor errors EPR spectra of nanodiamond samples as well as of the TEMPO standard were registered together with a Mn^{2+}/MgO sample placed in the same resonator. The accuracy of the g-factor determination was estimated to be ±0.0002. The concentration of radicals was determined according to [27] by a comparison of the double integral of the EPR-spectrum, divided by the amplitude of the EPR-spectrum of a secondary standard (Cr^{3+} in ruby), with the corresponding value for a weighted sample of TEMPO. The accuracy of the determination of the radical concentration was estimated to be ±10%.

Pulse EPR measurements were made on a Bruker E580 spectrometer. Echo-detected EPR spectra were recorded as the intensity of the simple Hahn echo depending on the magnetic field. Spin–lattice (T_1) relaxation times were measured by using the inversion recovery pulse sequence (π–T–$\pi/2$–τ–$\pi/2$–τ–echo). Spin–spin (T_2) relaxation times were measured by using the simple Hahn echo sequence ($\pi/2$–τ–π–τ–echo). The value of tau was 180 or 200 ns. Both values gave similar results. Details on the treatment of pulse spectra as well as on the measurements of relaxation times can be found in [28].

All EPR measurements were made at room temperature.

EPR spectra were registered in the presence of air over the sample as well as after air evacuation by rotary pump up to 1.3 Pa (10^{-2} torr). The reversible influence of air on the relaxation times has been confirmed by opening of the evacuated sample to air and repeated evacuation followed by pulse EPR measurements after each procedure.

Simulation of the EPR-spectrum of the P1-center in nanodiamond was made by an automatic fitting method described in [29].

3. Results and discussion

Both nanodiamond samples had intensive EPR spectra at g = 2.0025 ± 0.0002 (Fig. 1, spectra 1 and 3). These spectra had a Lorentz line shape with peak-to-peak width ΔH_{pp} = 0.95 ± 0.05 mT. The spin concentration was 8×10^{19} spins/g for ND#1 and 7×10^{19} spins/g for ND#2. The presence of air as well as of vacuum 1.3 Pa over the samples did not influence on the shape and intensity of EPR spectra (in the range ±10%). Data on the g-factor as well as on the concentration of paramagnetic centers are consistent with the literature within the experimental errors [5,8,9]. According to recent NMR data [10,11], these paramagnetic centers are located mainly in the bulk.

In pulse EPR measurements, the spin echo signal at g = 2.0025 was almost negligible. This result may be explained by short relaxation times of the paramagnetic centers [8] which did not give echoes under the experimental conditions. Registration of echo-detected EPR-spectrum at room temperature together with prolonged accumulation (overnight) allowed to get good patterns of the P1-center (Fig. 1, spectra 2 and 4) without the broad line corresponding to other radicals as observed previously at low temperatures [18,19].

The best simulation of the P1-center spectrum (Fig. 2, spectra 1 and 2) has been achieved with h.f.s. parameters A_{xx} = 2.57 mT, A_{yy} = 3.08 mT, A_{zz} = 4.07 mT. EPR spectra of a P1-center with axial h.f.s. tensor have been observed previously in diamond crystals [30,31], in polycrystalline diamond films [32,33] and in carbonado [34]. According to [32], the internal stress caused the distortion of axial symmetry of the P1-center in some CVD diamond films. The slight deviation from an axial symmetry of the h.f.s. tensor of the
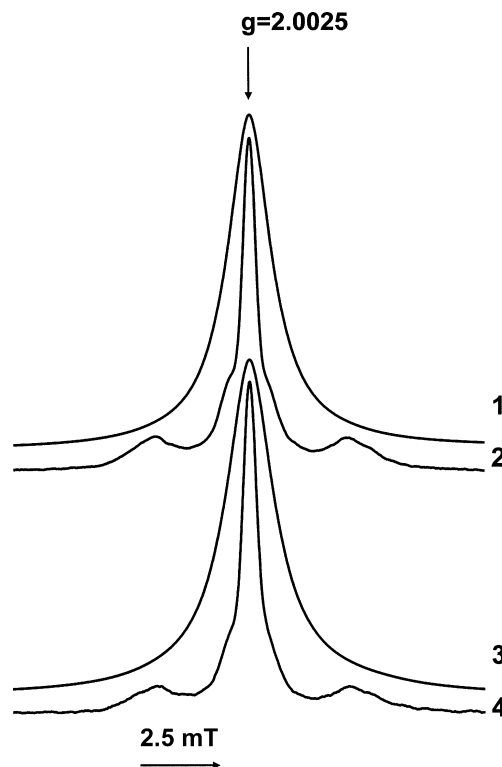

Fig. 1. Normalized EPR spectra of detonation nanodiamonds: 1 and 3 – CW EPR (in integral form); 2 and 4 – echo-detected EPR; 1 and 2 – ND#1 sample; 3 and 4 – ND#2 sample.

P1-centers in the nanodiamond observed in the present work also may be explained by a distortion of the diamond lattice. Our data are consistent with the model of nanodiamond proposed in [35,36]. According to [35,36], there is a core with a perfect diamond lattice which is surrounded by a shell of compressed diamond lattice, and this core–shell structure is enveloped in a non-diamond carbon. Recent NMR data [11] showed the presence of nitrogen atoms in the shell of nanodiamond particle, not in the core. It is possible to propose that the P1-centers are located in the compressed diamond shell. However the possibility of the distortion of the nanodiamond core caused by a small size of the crystallites can not be excluded completely. For the annealed detonation nanodiamond with larger crystallites size the distortion of the P1-centers has not been reported [20]. Therefore the distortion of the P1-centers is typical only for the smallest size of nanodiamond crystallites. The question on the presence or absence of P1-centers in the nanodiamond core as well as in the shell requires additional investigations.

Other spectra are overlapped and are difficult to be analyzed (Fig. 2, spectrum 3). Taking into account the EPR data on CVD diamond films [37,38] the spectrum 3 of the Fig. 2 may be interpreted as the superposition of the spectrum from the H1-center (the defect in diamond lattice containing one hydrogen atom, g = 2.0028) and the single line (g = 2.0025, ΔH_{pp} = 0.40 ± 0.05 mT) from other centers. It is worth to note that radicals of the crystal diamond surface have similar parameters (g = 2.0025–2.0027, ΔH_{pp} = 0.5–0.6 mT) [39–42]. The oxygen effect is well-known for surface radicals of carbon [43]. A slight influence of ambient oxygen on the relaxation times T_1 and T_2 measured at the central field position (Table 1) allowed us to propose that the single line spectrum can be due to the surface radicals, probably carbon dangling bonds. Both P1-centers and H1-centers are bulk defects and therefore do not have to interact with the ambient oxygen. The concen-
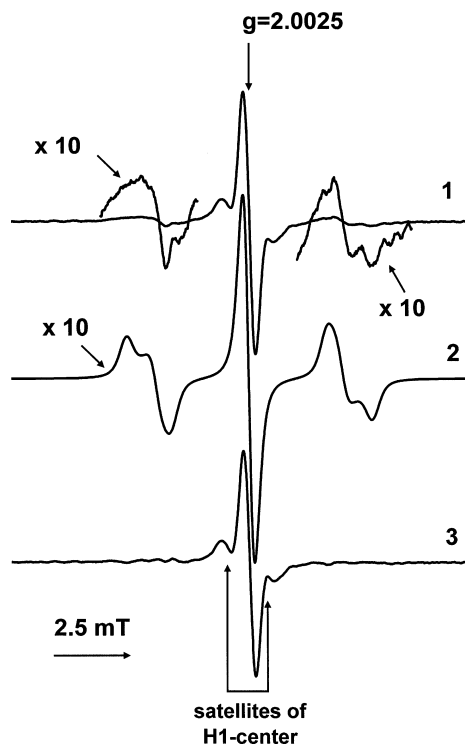
Fig. 2. 1 – First derivative of echo-detected EPR-spectrum of ND#1 sample; 2 – model spectrum with parameters ($g = 2.0025$, nuclear spin = 1, $A_{xx} = 2.57$ mT, $A_{yy} = 3.08$ mT, $A_{zz} = 4.07$ mT, Voigt line shape with $\Delta H_{pp} = 4.0$ G and Lorentzian/Gaussian line-width ratio equal to 1.0); 3 – result of subtraction of 2 from 1.

Table 1
Relaxation times T_1 and T_2 (μs, ±10%) of radical species in the detonation nanodiamonds exposed to air and under vacuum 1.3 Pa (measured by pulse EPR at the central field position).

Sample	T_1 (air)	T_1 (vacuum)	T_2 (air)	T_2 (vacuum)
ND#1	1.6	1.9	0.11	0.13
ND#2	1.8	2.1	0.13	0.17

tration of surface radicals is very low in comparison with the concentration of bulk radicals and is difficult to be measured. However surface radicals are not absent completely in the detonation nanodiamonds.

The detection of the P1-centers spectrum by pulse EPR means that a similar spectrum has to be present in CW EPR [18]. However the intensive broad line from bulk radicals (Fig. 3, spectra 1 and 2) prevented to detect it. The problem was how to simulate [44] and subsequently subtract this broad line to see the spectrum of P1-centers. We have found that fitting of the broad line by the mixed Lorentz + Gauss derivative line (XEPR software) gave good results (Fig. 3, spectra 1′ and 2′). The difference spectra contained patterns corresponding to the P1-centers, which have been detected also by pulse EPR (Fig. 2).

The central part of the difference spectra (Fig. 3, spectra 3 and 4) showed three lines. The distance between these lines increased with the increase of the microwave power. Therefore these lines may not be interpreted as a real spectrum and might arise due to the imperfection of the fitting. The question about the best fitting of the spectrum of bulk radicals requires additional investigation.

Lines corresponding to the P1-center do not arise from the imperfection of the spectrum fitting and can be used for the estimation of the concentration of paramagnetic nitrogen. It has been reported [17] that the concentration of paramagnetic nitrogen in detonation nanodiamonds is less than 10 ppb. We have found that
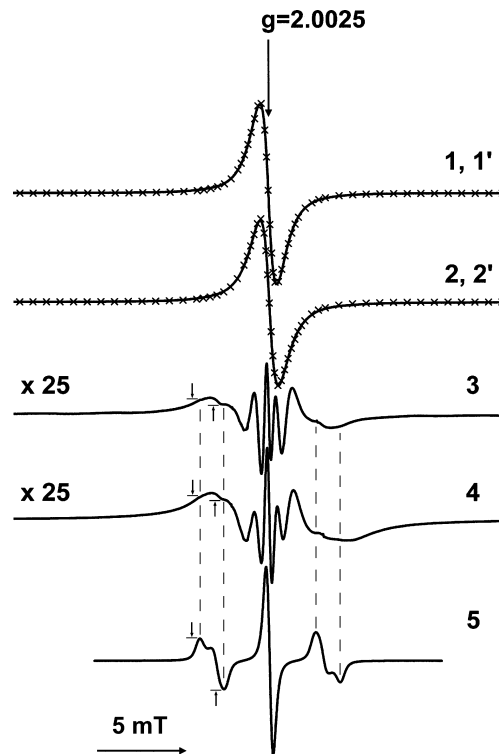
Fig. 3. CW EPR spectra of detonation nanodiamonds: 1 – ND#1 sample; 2 – ND#2 sample; 1′ and 2′ (markers) – fitted spectra for 1 and 2, respectively; 3 – result of subtraction of 1′ from 1; 4 – result of subtraction of 2′ from 2; 5 – model spectrum of P1-center (the same that in Fig. 2, spectrum 2). Arrows show the amplitude of the $m_I = +1$ line of the P1-center spectrum.
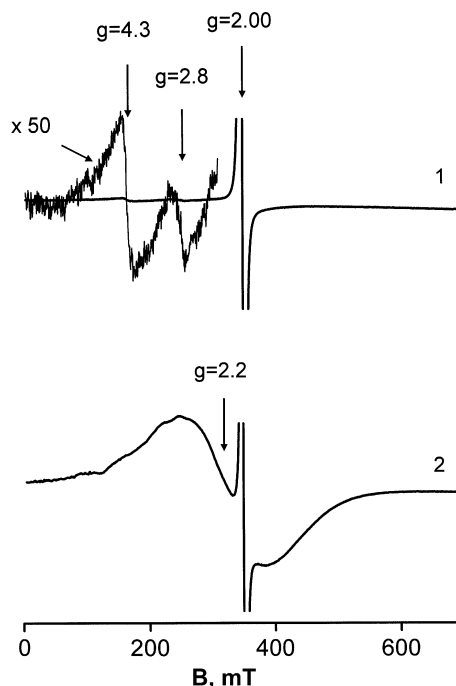
Fig. 4. Broad range CW EPR spectra of detonation nanodiamonds: 1 – ND#1 sample; 2 – ND#2 sample. Spectra registered at microwave power 200 mW, microwave frequency 9.79 GHz, modulation amplitude 0.1 mT, modulation frequency 100 kHz. EPR-spectrum at $g = 2.0$ is assigned to the radical-like paramagnetic centers [5], at $g = 4.3$ – to the Fe^{3+} ions situated in a non-crystalline phase [45], at $g = 2.8$ – to the background signal of empty resonator and a broad line at $g = 2.2$ – to the ferromagnetic resonance of Fe, Co or Ni [8].

the concentration of P1-centers is larger. With the use of the model spectrum (Fig. 3, spectrum 5), we have estimated the concentration of P1-centers as $(8 \pm 4) \times 10^{16}$ centers/g or 2 ± 1 ppm N. Taking into account a total content of nitrogen of 2 wt.% or 2×10^4 ppm [13], it is possible to conclude that only a fraction part of 10^{-4} of the nitrogen in detonation nanodiamond is in P1-centers.

According to broad range EPR spectra (Fig. 4) the ND#2 sample contained more transition metal impurities than the ND#1 sample. However both nanodiamond samples gave similar CW and pulse EPR spectra (see Fig. 1). Therefore we have not found the influence of the transition metal impurities on the structure and the concentration of the P1-centers, H1-centers and radicals.

4. Conclusion

The detonation nanodiamonds contain distorted P1-centers, H1-centers and radicals located mainly in the bulk. The spectrum of bulk radicals ($g = 2.0025 \pm 0.0002$, a Lorentz line shape with $\Delta H_{pp} = 0.95 \pm 0.05$ mT) dominates in CW EPR and prevents to record spectra from other paramagnetic species. The bulk radicals are not manifested in pulse EPR because of short relaxation times. The pulse EPR-spectrum is composed of lines due to P1-centers with parameters ($g = 2.0025$, $A_{xx} = 2.57$ mT, $A_{yy} = 3.08$ mT, $A_{zz} = 4.07$ mT), H1-centers ($g = 2.0028$) and a single line ($g = 2.0025$, $\Delta H_{pp} = 0.40 \pm 0.05$ mT) from other centers which may be assigned to surface radicals because of the observed influence of ambient oxygen on the relaxation times measured by pulse EPR. EPR data are consistent with the core–shell model of the detonation nanodiamond. The concentration of P1-centers is estimated by CW EPR as $(8 \pm 4) \times 10^{16}$ centers/g or 2 ± 1 ppm N. Transition metal impurities did not influence on the structure and the concentration of the P1-centers, H1-centers and radicals in the samples under study.

Acknowledgement

References

[1] H.O. Dean (Ed.), Nanodiamonds: Applications in Biology and Nanoscale Medicine, Springer, New York-Dordrecht-Heidelberg-London, 2010, p. 288.
[2] M. Baidakova, A. Vul, J. Phys. D: Appl. Phys. 40 (2007) 6300.
[3] E. Ōsawa, Pure Appl. Chem. 80 (2008) 1365.
[4] V.Yu. Dolmatov, J. Superhard Mater. 31 (2009) 158.
[5] A.I. Shames et al., J. Phys. Chem. Solids 63 (2002) 1993.
[6] V.Yu. Osipov, A.I. Shames, T. Enoki, K. Takai, M.V. Baidakova, A.Ya. Vul', Diamond Relat. Mater. 16 (2007) 2035.
[7] V.Yu. Osipov, A.I. Shames, A.Ya. Vul', Physica B 404 (2009) 4522.
[8] A.I. Shames, A.M. Panich, W. Kempiński, M.V. Baidakova, V.Yu. Osipov, T. Enoki, A.Ya. Vul', in: D.M. Gruen, O.A. Shenderova, A.Ya. Vul' (Eds.), Synthesis, Properties and Applications of Ultrananocrystalline Diamond, NATO Science Series II: Mathematics, Physics and Chemistry, vol. 192, Springer, Netherlands, 2005, p. 271.
[9] A.I. Shames et al., Diamond Relat. Mater. 16 (2007) 1806.
[10] M. Dubois et al., J. Phys. Chem. C 113 (2009) 10371.
[11] X. Fang, J. Mao, E.M. Levin, K. Schmidt-Rohr, J. Am. Chem. Soc. 131 (2009) 1426.
[12] O. Madelung, U. Rössler, M. Schulz, Impurities and defects in group IV elements, IV–IV and III–V compounds. Part a: group IV elements, in: Landolt-Börnstein (Ed.), Numerical Data and Functional Relationships in Science and Technology – New Series, Group III Condensed Matter, vol. 41A2a, 2002, p. 877.
[13] A. Krüger et al., Carbon 43 (2005) 1722.
[14] A.S. Barnard, M. Sternberg, Diamond Relat. Mater. 16 (2007) 2078.
[15] C. Bradac, T. Gaebel, N. Naidoo, J.R. Rabeau, A.S. Barnard, Nano Lett. 9 (2009) 3555.
[16] K. Iakoubovskii, G.J. Adriaenssens, K. Meykens, M. Nesladek, A.Y. Vul, V.Y. Osipov, Diamond Relat. Mater. 8 (1999) 1476.
[17] K. Iakoubovskii, M.V. Baidakova, B.H. Wouters, A. Stesmans, G.J. Adriaenssens, A.Ya. Vul', P.J. Grobet, Diamond Relat. Mater. 9 (2000) 861.
[18] B.R. Smith et al., Small 5 (2009) 1649.
[19] A.A. Soltamova et al., Phys. B: Condens. Matter 15 (2009) 4518.
[20] P.G. Baranov et al., JETP Lett. 89 (2009) 409.
[21] N.N. Rozhkova, L.E. Gorlenko, G.I. Emel'yanova, A. Jankowska, M.V. Korobov, V.V. Lunin, E. Osawa, Pure Appl. Chem. 81 (2009) 2093.
[22] E.V. Golubina, S.A. Kachevsky, E.S. Lokteva, V.V. Lunin, P. Canton, P. Tundo, Mendeleev Commun. 19 (2009) 133.
[23] E. Ōsawa, Diamond Relat. Mater. 16 (2007) 2018.
[24] A.M. Panich, A.I. Shames, H.-M. Vieth, E. Ōsawa, M. Takahashi, A.Ya. Vul', Eur. Phys. J. B 52 (2006) 397.
[25] S.I. Chukhaeva, P.Ya. Detkov, A.P. Tkachenko, A.D. Toropov, Sverkhtverd. Mater. (4) (1998) 29.
[26] Ya.S. Lebedev, O.Ya. Grinberg, A.A. Dubinsky, O.G. Poluektov, in: R.I. Zhdanov (Ed.), Bioactive Spin Labels, Springer-Verlag, Berlin-Heidelberg-New York, 1992, p. 227.
[27] C.P. Poole, Electron Spin Resonance: A Comprehensive Treatise on Experimental Techniques, Wiley, New York, 1983.
[28] M. Brustolon, A. Barbon, in: A. Lund, M. Shiotani (Eds.), EPR of Free Radicals in Solids – Trends in Methods and Applications, Kluwer Academic Publishers, Dordrecht/Boston/London, 2003, p. 39.
[29] A. Lund, Appl. Magn. Reson. 26 (2004) 365.
[30] W.V. Smith, P.P. Sorokin, I.L. Gelles, G.J. Lasher, Phys. Rev. 115 (1959) 1546.
[31] C. Kedkaew, P. Limsuwan, K. Thongcham, S. Meejoo, Int. J. Mod. Phys. B 22 (2008) 4740.
[32] K. Iakoubovskii, A. Stesmans, G.J. Adriaenssens, R. Provoost, R.E. Silverans, V. Raiko, Phys. Status Solidi A 174 (1999) 137.
[33] T.A. Karpukhina, L.L. Bouilov, V.F. Chuvaev, Surf. Coat. Technol. 47 (1991) 538.
[34] R.M. Mineeva, A.V. Speranskii, B.L. Egorov, L.V. Bershov, M.V. Chukichev, Geochem. Int. 38 (2000) 121.
[35] B. Palosz, C. Pantea, E. Grzanka, S. Stelmakh, Th. Proffen, T.W. Zerda, W. Palosz, Diamond Relat. Mater. 15 (2006) 1813.
[36] B. Palosz, S. Stelmakh, E. Grzanka, S. Gierlotka, W. Palosz, Z. Kristallogr. 222 (2007) 580.
[37] X. Zhou, G.D. Watkins, K.M. McNamara Rutledge, R.P. Messmer, S. Chawla, Phys. Rev. B 54 (1996) 7881.
[38] D.F. Talbot-Ponsonby, M.E. Newton, J.M. Baker, G.A. Scarsbrook, R.S. Sussmann, A.J. Whitehead, S. Pfenninger, Phys. Rev. B 57 (1998) 2264.
[39] J.H.N. Loubster, J.A. van Wyk, Rep. Prog. Phys. 41 (1978) 1201.
[40] N.D. Samsonenko, G.V. Zhmykhov, V.Sh. Zon, V.K. Aksenov, J. Struct. Chem. 20 (1979) 951.
[41] S.I. Gorbachuk, N.G. Kakazei, V.S. Kardasevich, V.N. Minakov, G.A. Podryazei, B.I. Reznik, Yu.M. Rotner, Soviet Powder Metall. Met. Ceram. 30 (1991) 669.
[42] E.P. Smirnov, O.K. Semchinova, A.M. Abyzov, D. Uffmann, Carbon 35 (1997) 31.
[43] D.J.E. Ingram, Biological and Biochemical Applications of Electron Spin Resonance, Adam Hilger Ltd., London, 1969.
[44] A.M. Panich, H.-M. Vieth, A.I. Shames, N. Froumin, E. Ōsawa, A. Yao, J. Phys. Chem. C 114 (2010) 774.
[45] S. Simon, J. Optoelectron. Adv. Mater. 8 (2006) 99.